Dimerization and phosphorylation of Lutheran/basal cell adhesion molecule are critical for its function in cell migration on laminin

Received for publication, January 18, 2019, and in revised form, July 2, 2019 Published, Papers in Press, August 14, 2019, DOI 10.1074/jbc.RA119.007521

Anna Guadall[‡§¶1], Sylvie Cochet[‡§¶1], Olivier Renaud[‖**‡‡§§], Yves Colin[‡§¶], Caroline Le Van Kim[‡§¶], Alexandre G. de Brevern[‡§¶], and Wassim El Nemer[‡§¶2]

*From the [‡]Université de Paris, UMR_S1134, BIGR, Inserm, F-75015 Paris, France, [§]Institut National de la Transfusion Sanguine, F-75015 Paris, France, [¶]Laboratoire d'Excellence GR-Ex, 75015 Paris, France, [‖]Institut Curie, Paris Sciences et Lettres Research University, 75005 Paris, France, **U934, Institut National de la Santé et de la Recherche Médicale, 75005 Paris, France, [‡‡]UMR3215, Centre National de la Recherche Scientifique , 75005 Paris, France, and [§§]Cell and Tissue Imaging Facility (PICT-IBiSA), Institut Curie, 75005 Paris, France*

Edited by Peter Cresswell

Tumor cell migration depends on the interactions of adhesion proteins with the extracellular matrix. Lutheran/basal cell adhesion molecule (Lu/BCAM) promotes tumor cell migration by binding to laminin α5 chain, a subunit of laminins 511 and 521. Lu/BCAM is a type I transmembrane protein with a cytoplasmic domain of 59 (Lu) or 19 (Lu(v13)) amino acids. Here, using an array of techniques, including site-directed mutagenesis, immunoblotting, FRET, and proximity-ligation assays, we show that both Lu and Lu(v13) form homodimers at the cell surface of epithelial cancer cells. We mapped two small-*XXX*-small motifs in the transmembrane domain as potential sites for monomers docking and identified three cysteines in the cytoplasmic domain as being critical for covalently stabilizing dimers. We further found that Lu dimerization and phosphorylation of its cytoplasmic domain were concomitantly needed to promote cell migration. We conclude that Lu is the critical isoform supporting tumor cell migration on laminin 521 and that the Lu:Lu(v13) ratio at the cell surface may control the balance between cellular firm adhesion and migration.

Lutheran/basal cell adhesion molecule (Lu/BCAM),[3] or CD239, is a type I transmembrane protein carrying the antigens of the Lutheran blood group system. Lu/BCAM is a member of the immunoglobulin superfamily (IgSF); it exhibits an extracellular domain composed of two variable (V) and three constant (C2) Ig-like domains, a single transmembrane domain, and a cytoplasmic domain of 59 or 19 amino acids that defines the two Lu/BCAM isoforms Lu (85 kDa) and Lu(v13) (78 kDa), respectively.

Lu/BCAM was first reported in circulating red blood cells (RBCs) through the presence of the Lutheran blood group antigens, but it is not restricted to the erythroid lineage because it has a broad expression pattern including epithelial and endothelial cells of most organs. Lu/BCAM binds to α5 chain–containing laminins and is the unique laminin receptor on the surface of circulating RBCs in humans (1–3). The adhesive function of Lu/BCAM has been studied mainly in the context of blood and lysosomal pathologies (4), such as sickle cell disease (5–9), hereditary spherocytosis (10), myeloproliferative neoplasms (11–13), and Gaucher disease (14), and to a lesser extent in epithelial cells and tumor invasion or metastasis.

Metastasis is often initiated and supported by the ability of tumor cells to invade the basement membrane through a cooperative process extracellular matrix (ECM) degradation, cell adhesion, and cell migration. The ECM protein laminin is believed to play a central role in cell adhesion and cell migration during tumor invasion. Laminins are heterotrimeric glycoproteins composed of α, β, and γ chains. There are five α chains, three β chains, and three γ chains (15), the combination of which gives rise to 19 different isoforms in the laminin family (16).

BCAM was first identified as an overexpressed antigen in human ovarian carcinomas *in vivo* that was up-regulated following malignant transformation (17, 18). Rahuel *et al.* (19) later demonstrated that BCAM and Lutheran were two splice variants (Lu(v13) and Lu, respectively) encoded by the *LU* gene. Since then, Lu/BCAM expression has been studied in a number of cancer cells and found modulated in several cancer types such as colon, skin, brain, liver, thyroid, breast, and bladder cancer (2, 20–28). Lu/BCAM has been shown to sustain tumor cell migration by modulating integrin-mediated cell attachment to laminin 511 (29) and to play a role in metastatic spreading of KRAS-mutant colorectal cancer (30).

In this study, we investigated the nature of Lu/BCAM molecules expressed at the membrane of epithelial cancer cells and revealed the presence of homodimers. We mapped two

This study was supported by the French National Research Agency through the "Investissements d'avenir" Program, France-BioImaging, ANR-10-INBS-04 and by Laboratory of Excellence GR-Ex Grant, reference ANR-11-LABX-0051. The labex GR-Ex is funded by the program "Investissements d'avenir" of the French National Research Agency, reference ANR-11-IDEX-0005-02. The authors declare that they have no conflicts of interest with the contents of this article.

This article contains Figs. S1–S3 and Videos S1–S9.

[1] These authors contributed equally to this work.

[2] To whom correspondence should be addressed. Tel.: 331-4449-3071; Fax: 331-4306-5019; E-mail: wassim.el-nemer@inserm.fr.

[3] The abbreviations used are: Lu/BCAM, Lutheran/basal cell adhesion molecule; ANOVA, analysis of variance; Cer, cerulean; Cit, citrine; ECM, extracellular matrix; IgSF, immunoglobulin superfamily; LIPS, LIPid-facing Surface; MDCK, Madin-Darby canine kidney cells; RBCs, red blood cells; PBS-CM, PBS with 1 mM calcium and magnesium; PLA, proximity ligation assay.

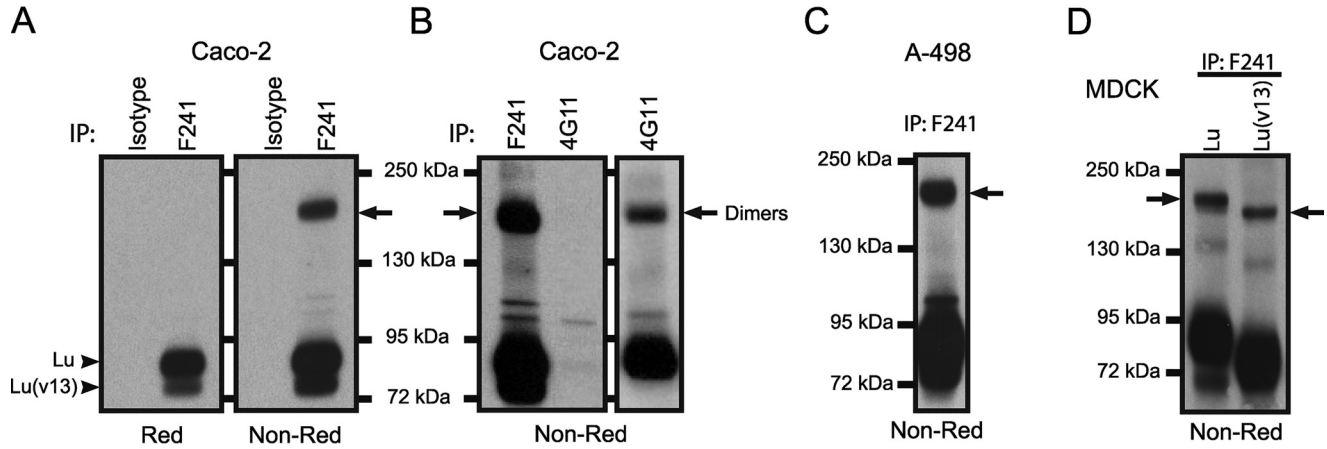

Figure 1. Lu/BCAM forms homodimers at the surface of epithelial cells. *A–D*, Lu/BCAM was immunoprecipitated from Caco-2 (*A* and *B*), A-498 (*C*), or transfected MDCK (*D*) epithelial cells using the F241 anti-human Lu mAb with or without biotinylation of surface proteins. SDS-PAGE was performed under reducing (*Red*) or nonreducing (*Non-Red*) conditions. Proteins were revealed using streptavidin-HRP. *A*, biotinylated endogenous Lu (85 kDa) and Lu(v13) (78 kDa) monomers are immunoprecipitated from Caco-2 cells ($n = 7$). An extra 170–175 kDa band corresponding to putative Lu dimers is visible under Non-Red conditions. *B*, *left panel*, biotinylated lysates containing endogenous Lu/BCAM isoforms with the Lu^b antigen specificity were mixed with nonbiotinylated lysates containing recombinant Lu isoform with the antithetical Lu^a antigen specificity. Immunoprecipitation was performed with F241 or 4G11 anti-Lu^a mAbs. *B*, *right panel*, immunoprecipitation of biotinylated recombinant Lu^a allelic variant using 4G11 mAb ($n = 1$). *C*, immunoprecipitation of biotinylated endogenous Lu and Lu(v13) in A-498 cells using F241 mAb ($n = 2$). *D*, immunoprecipitation of biotinylated recombinant Lu and Lu(v13) in transfected MDCK cells using F241 mAb ($n = 7$). *Arrows* indicate dimers. *IP*, immunoprecipitation.

small-*XXX*-small motifs in the transmembrane domain as potential sites for monomers docking and identified three cysteines in the cytoplasmic domain as critical residues for dimers' covalent stabilization. Finally, we showed that dimerization of Lu/BCAM together with the phosphorylation of its cytoplasmic domain at serine 621 are critical factors to promote cell migration on laminin 521.

Results

Lu/BCAM forms homodimers at the surface of epithelial cells

To study the nature of Lu/BCAM molecules at the cell membrane, surface proteins of Caco-2 cells, a human epithelial colorectal carcinoma cell line, were biotinylated before cell lysis and Lu/BCAM was immunoprecipitated using the F241 anti-human Lu/BCAM mAb. After SDS-PAGE and transfer to nitrocellulose membrane, immunoprecipitated proteins were revealed using streptavidin-HRP. Under nonreducing conditions, a band of 170–175 kDa was detected in addition to the expected Lu/BCAM isoforms Lu (85 kDa) and Lu(v13) (78 kDa) (Fig. 1*A*). This band was not detected in the presence of a reducing agent (β-mercaptoethanol) and no proteins other than Lu and Lu(v13) were detected in these conditions, suggesting that the 170–175 kDa band represented a dimer of Lu/BCAM that was reduced to the monomeric size by β-mercaptoethanol (Fig. 1*A*). To test whether these potential dimers were not forming *in vitro* after cell lysis, immunoprecipitation experiments were performed after mixing two populations of Lu/BCAM proteins with antithetical antigen specificities: Lu^a and Lu^b. Caco-2 cell lysates containing biotinylated Lu/BCAM with the Lu^b antigen (biotin-Lu^b) were mixed with nonbiotinylated lysates of Caco-2–Lu^a cells expressing a recombinant form of Lu/BCAM with the Lu^a antigen (31). Immunoprecipitation of Lu^a using the 4G11 anti-Lu^a mAb did not show any biotinylated band at the dimer size (Fig. 1*B*, *left panel*) indicating that no Lu^a/biotin-Lu^b dimers were forming *in vitro* during the purification step. This was not due to the inability of 4G11 mAb to immunoprecipitate Lu dimers because such dimers were detected when surface proteins of Caco-2–Lu^a cells were biotinylated (Fig. 1*B*, *right panel*).

To test whether dimer formation was restricted to Caco-2 cells, similar immunoprecipitation experiments using the A-498 human renal epithelial cell line were performed. The presence of Lu/BCAM dimers was also detected in these cells (Fig. 1*C*) indicating that this was not exclusive to Caco-2 cells.

Because Lu(v13) is weakly expressed in Caco-2 and A-498 cells it was not possible to detect Lu(v13) dimers in our experiments. To test if Lu and Lu(v13) are both able to form dimers, Madin-Darby canine kidney cells (MDCK) were transfected to generate stable cell lines that express either of the two human isoforms. In both cases, a high molecular weight band corresponding to the putative dimers was observed after biotinylation and immunoprecipitation with F241 mAb (Fig. 1*D*). As expected, the Lu and Lu(v13) dimers were different in size because of the 40 amino acid difference between the two monomers.

Lu homodimers are detected at the cell surface by FRET

Lu homodimerization in living cells was assessed by FRET assays using HEK 293T cells. HEK 293T cells were cotransfected with vectors encoding the fluorophores cerulean (Cer) or citrine (Cit) fused to the C terminus of the long Lu isoform (pE-Lu-Cer and pE-Lu-Cit). Positive and negative controls were performed: A vector encoding a Cit-Cer tandem (pE-Cit-Cer, positive control), cotransfection of a vector encoding Cit (pE-Cit) with a vector encoding Cer (pE-Cer), cotransfection of pE-Lu-Cit and pE-Cer vectors, and cotransfection of pE-Lu-Cit vector with a vector encoding an independent transmembrane protein of the IgSF (ICAM4) fused to Cer (pE-ICAM4-Cer). The Cer/Cit fluorophore pair was selected for its good spectral overlap allowing for efficient energy transfer from the donor (Cer) to the acceptor (Cit). The transfer of energy was measured as an increase in the donor fluorophore emission after photo-

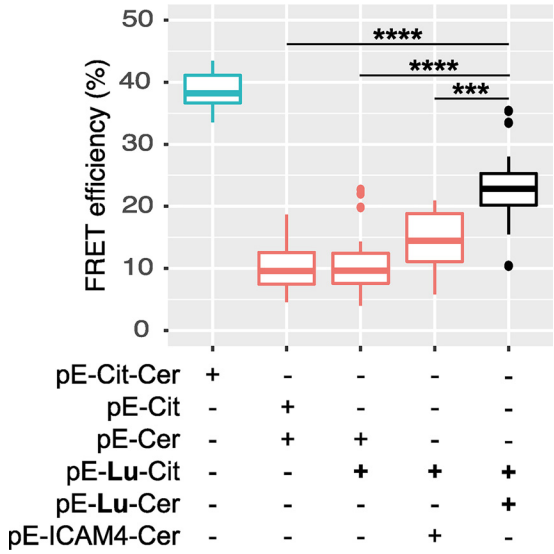

Figure 2. The fusion proteins Lu-Cit and Lu-Cer form homodimers at the cell surface that are detected by FRET. FRET efficiency in transiently transfected HEK 392T cells of the tandem pE-Cit-Cer fusion protein (positive control; *green*), three negative controls (pE-Cit + pE-Cer, pE-Lu-Cit + pE-Cer, and pE-Lu-Cit + pE-ICAM4-Cer; *red*), and pE-Lu-Cit + pE-Lu-Cer combination. Kruskal-Wallis one-way ANOVA on ranks test was performed followed by Dunn's multiple comparison procedure in case of differences at a 0.05 significance level. Significant differences between the pE-Lu-Cit + pE-Lu-Cer cotransfectant and the negative controls are shown: ***, $p \leq 0.001$; ****, $p \leq 0.0001$ (tandem, $n = 26$; pE-Cit + pE-Cer and pE-Lu-Cit + pE-Cer, $n = 28$; pE-Lu-Cit + pE-ICAM4-Cer, n = 27; pE-Lu-Cit + pE-LuCer, $n = 35$). The energy transfer between Lu-Cer and Lu-Cit and the negative control pE-Lu-Cit + pE-ICAM4-Cer has been assessed in two additional independent experiences.

bleaching of the acceptor. Fig. S1 shows representative images of the photobleaching process on an area where Lu-Cit is expressed. FRET efficiency of the cells expressing the Cit/Cer or the Lu-Cit/Cer pair was much lower than that of those expressing the Cit-Cer tandem (positive control) used to determine the maximal FRET efficiency that could be obtained in this system (38.6 ± 2.6%, mean ± S.D.; Fig. 2). The FRET efficiency of the Cit/Cer pair was not null, indicating that there was some background because of a crosstalk between the two overexpressed fluorescent proteins. The FRET efficiency of cells co-expressing Lu-Cit and Lu-Cer was significantly higher than that of cells expressing the Cit/Cer or the Lu-Cit/Cer pair (negative controls), indicating that Lu molecules interact with each other at the cell membrane and form homodimers or homooligomers (Fig. 2). The measured FRET efficiency of Lu dimers was not subsequent to Lu overexpression at the cell membrane because it was greater than the efficiency of Lu-Cit co-expressed with ICAM4-Cer, another IgSF transmembrane protein that does not interact with Lu (pE-Lu-Cit + pE-ICAM4-Cer; Fig. 2).

Mapping of Lu/BCAM dimerization site

Analysis of the primary sequence of Lu/BCAM transmembrane domain revealed the presence of two overlapping "small-*XXX*-small" motifs: A553-*XXX*-S557 and A555-*XXX*-G559 (Fig. 3*A*). Small-*XXX*-small motifs are overrepresented in transmembrane proteins and well-known for promoting helix-helix interactions and protein oligomerization. Site-directed mutagenesis was performed to substitute serine 577 or glycine 559 by valine: LuS557V and LuG559V mutants. Immunoprecipitation assays performed after stable expression of these two mutants in MDCK cells did not show altered dimerization as compared with WT Lu (Fig. 3*B*).

Because dimerization was not suppressed by the S557V and G559V mutations, the role of disulfide bonds in Lu homodimers stabilization was investigated. This hypothesis is supported by the absence of homodimers when SDS-PAGE was performed under reducing conditions (Fig. 1*A*). There are 13 cysteines common to Lu and Lu(v13), 10 cysteines in the extracellular domain, and 3 in the cytoplasmic tail (Fig. 3*C*). We focused on the latter because Lu/BCAM isoforms exhibit five Ig-like extracellular domains involving the 10 other cysteines (Fig. 3*C*). The 3 cytoplasmic cysteines were mutated into serine or alanine as shown in Fig. 3*A*. The triple mutant LuC/S-CC/AA was stably expressed in MDCK cells and showed no dimers after immunoprecipitation (Fig. 3*B*), suggesting that the dimers of Lu WT detected by SDS-PAGE under nonreducing conditions were covalently linked by disulfide bonds involving cysteines of the cytoplasmic domain.

The impact of these mutations was further investigated using the proximity ligation assay (PLA) to assess Lu dimerization *in situ* at the cell surface, without the interference of the cell lysis and protein purification steps. Indeed, the triple mutant might form noncovalently linked dimers at the cell surface that are broken apart by the detergent at the lysis step before protein immunoprecipitation. Anti-Lu F241 antibody was purified and conjugated to the DNA oligo arms PLA-MINUS (F241-M) or PLA-PLUS (F241-P). MDCK cells were fixed and labeled with F241-M and F241-P antibodies. When close enough (<40 nm), the PLUS and MINUS oligo arms facilitate ligation, amplification, and subsequent fluorescent detection. In accordance with the FRET results, MDCK-Lu cells showed high numbers of fluorescent dots, supporting the presence of Lu dimers at the cell surface (Fig. 3, *D* and *E*). Similar results were obtained with the MDCK-LuS557V and -LuG559V cells, in accordance with the immunoprecipitation results. The number of fluorescent dots was decreased in MDCK cells expressing the triple mutant LuC/S-CC/AA, without reaching the background level measured with MDCK WT cells (Fig. 3*D* and 3*E*), indicating that the dimerization of this mutant was altered but not abolished at the cell surface, thus suggesting that disulfide bonds are not critical for dimerization to occur.

Lu homodimers promote cell migration

Lu/BCAM promotes migration of human fibrosarcoma cells through its interaction with laminin α5 chain (29). The potential role of Lu in inducing migration of MDCK cells was investigated by performing migration assays of individual MDCK cells spread onto a matrix of purified recombinant laminin 521 (Fig. S2). As expected for epithelial cells, MDCK WT cells were dynamic and showed basal migration activity (Fig. 4, *A* and *B*; Video S1). In accordance with Kikkawa's results using human fibrosarcoma cells, MDCK-Lu cells were more dynamic and showed a higher migration rate (Fig. 4, *A* and *B*; Video S2), with more than 2-fold increase when compared with MDCK WT (Fig. 4*B*). Migration of cells expressing Lu mutants LuS557V or LuG559V was also increased but to a lesser extent (Fig. 4, *A* and *B*; Videos S3 and S4). Migration of MDCK cells expressing LuC/

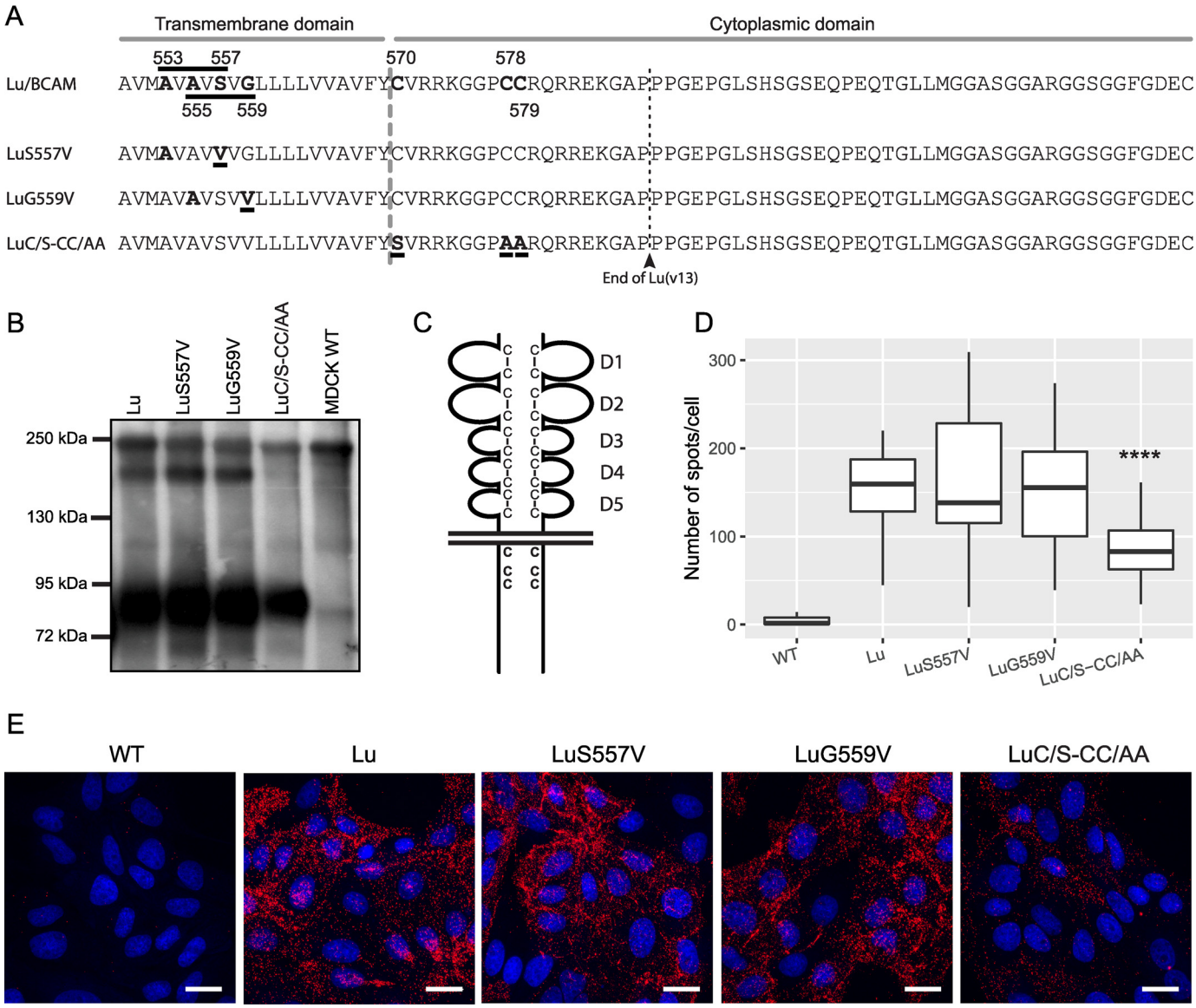

Figure 3. Mapping of Lu/BCAM dimerization sites. *A*, primary amino acid sequence of the transmembrane and cytoplasmic domains of Lu/BCAM and the three mutants LuS557V, LuG559V, and LuC/S-CC/AA. Substituted amino acids are *underlined* for each mutant. *B*, immunoprecipitated Lu and Lu mutants from transfected MDCK cells after biotinylation of surface proteins. SDS-PAGE was performed under nonreducing conditions; proteins were detected using streptavidin-HRP. The upper band of 250 kDa, detected in all cell types including MDCK WT, is a nonspecific band. LuS557V and LuG559V: $n = 7$; LuC/S-CC/AA: $n = 3$. *C*, schematic representation of two molecules of Lu/BCAM and the relative position of the 13 cysteines common to Lu and Lu(v13) isoforms. The 10 extracellular cysteines are involved in five Ig-like domains (D1-D5). *D*, boxplot showing the proximity ligation assay results obtained for MDCK WT and transfected MDCK cells expressing Lu or Lu mutants. Results are expressed as number of fluorescent dots per cell. Kruskal-Wallis one-way ANOVA on ranks test was performed for the transfected cells, followed by Dunn's multiple comparison procedure in case of differences at a 0.05 significance level. ****, $p \leq 0.0001$ *versus* MDCK-Lu cells (WT, $n = 14$; Lu and LuG559V, $n = 22$; LuS557V, $n = 19$; LuC/S-CC/AA, $n = 21$). This experiment has been performed three times. *E*, representative confocal microscopy images showing the PLA signal (*red*) on MDCK WT and transfected MDCK cells expressing Lu or Lu mutants; nuclei are stained with DAPI (*blue*). *Scale bar*: 20 μm.

S-CC/AA mutant was significantly diminished when compared with MDCK-Lu cells (Fig. 4, *A* and *B*; Video S5), suggesting that covalently linked homodimers are important for Lu-dependent cell migration.

Lu phosphorylation is essential for Lu-induced cell migration

Although Lu induced MDCK cell migration, Lu(v13) did not. As shown in Fig. 5, MDCK-Lu(v13) cells showed a similar behavior to MDCK WT cells (Video S6). Because Lu(v13) forms dimers at the MDCK cell surface (Figs. 1*D* and 5*C*), we concluded that dimerization alone was not sufficient to promote cell migration. Lu(v13) lacks 40 amino acids at the C-terminal end, when compared with Lu, among which the only serine residues of the cytoplasmic domain are found. Phosphorylation of serine 621 has been shown to activate Lu-mediated cell adhesion to laminin 511/521 (5, 11, 32). Therefore, we investigated the role of serine 621 phosphorylation in Lu-mediated cell migration by performing migration assays with stably transfected MDCK cells expressing a Lu mutant in which serine 621 was substituted by alanine (LuS621A). Migration of MDCK-LuS621A cells was strongly inhibited (Fig. 5, *A* and *B*; Video S7). This inhibition was not caused by altered dimerization because

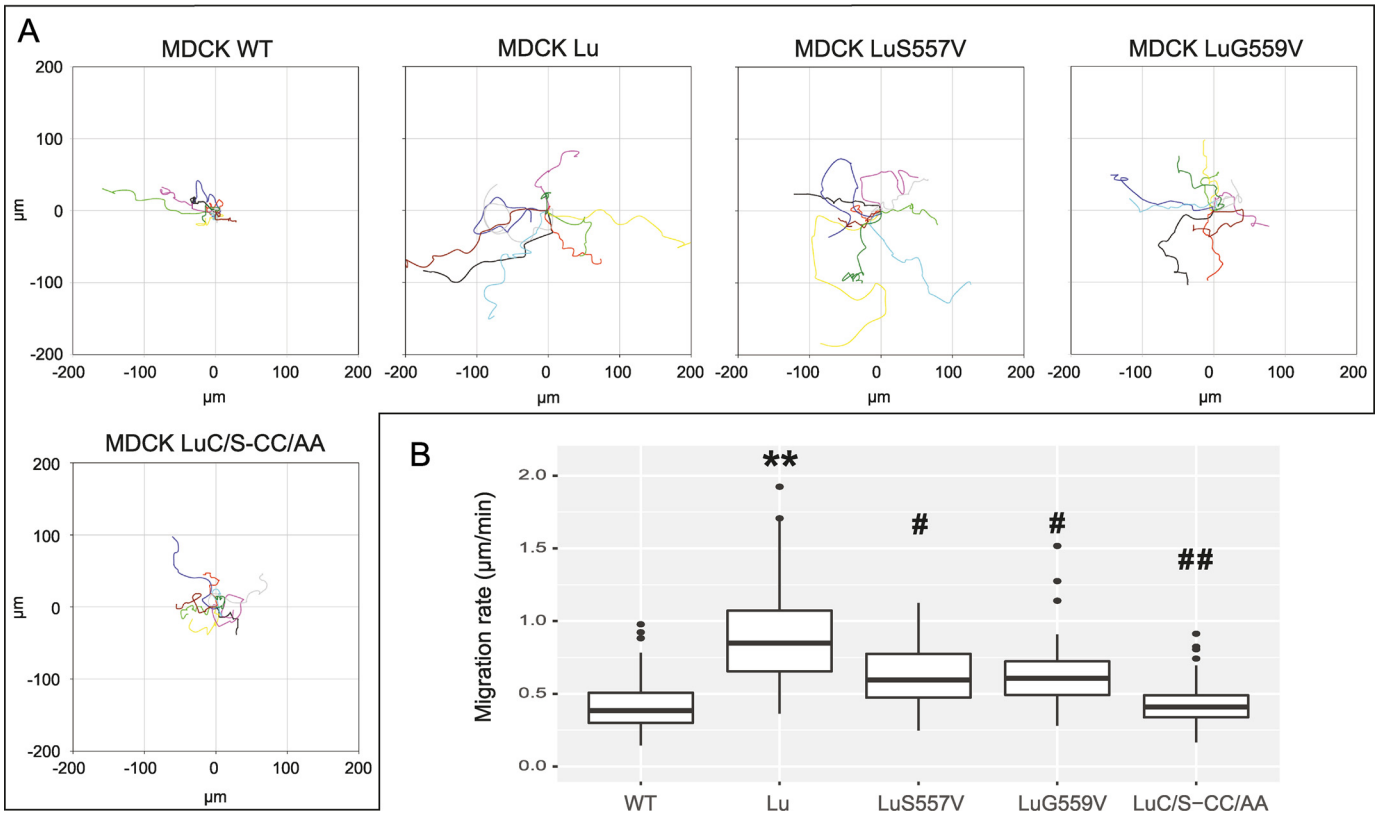

Figure 4. Lu homodimers sustain Lu-mediated cell migration. Indicated cells were plated in channels coated with laminin 521. Cell movements were monitored by time-lapse video microscopy. Cells were tracked for 12 h at 10 min intervals. *A*, representative tracks of 10 cells for each cell line over a span of 4 h. *B*, quantification of cell motility as evaluated by cell mean velocity (μm/min) on data collected from two independent experiments. ANOVA was performed on log-transformed data, followed by Tukey's honest significance test. **, $p \leq 0.01$ *versus* MDCK WT cells; #, $p \leq 0.05$ *versus* MDCK-Lu cells; ##, $p \leq 0.01$ *versus* MDCK-Lu cells (WT, $n_1 = 38$, $n_2 = 43$; Lu, $n_1 = 29$, $n_2 = 42$; LuS557V, $n_1 = 36$, $n_2 = 44$; LuG559V, $n_1 = 37$, $n_2 = 45$, LuC/S-CC/AA, $n_1 = 37$, $n_2 = 41$). Number of tracked cells of each cell line, for two independent experiments (n1 and n2).

LuS621A mutant showed normal levels of immunoprecipitated dimers (Fig. 5*C*). As serine 621 can be phosphorylated by PKA (32) or Akt (11), we performed migration assays in the presence of the PKA inhibitor H89 or the Akt inhibitor Akti. Migration of MDCK-Lu cells was significantly inhibited in the presence of H89 suggesting that it depended on Lu phosphorylation by PKA (Fig. 5*D*; Videos S8 and S9). Altogether, our results show that Lu-mediated cell migration on laminin 521 depends on concomitant dimerization and phosphorylation of Lu molecules at the cell surface.

Discussion

Although Lu/BCAM has been investigated for decades, it is the first time that its ability to form dimers at the cell surface is reported. These dimers were not detected previously because Western blotting experiments were performed under reducing conditions that are shown here to abolish dimerization.

Lu/BCAM binds to α5 chain–containing laminins and is the unique laminin receptor on the surface of circulating RBCs in humans (1–3). The binding site of Lu/BCAM to laminin was first mapped to the first three Ig-like extracellular domains (D1-D2-D3) (33), and then delimited to a negatively charged area in the D2-D3 interdomain flexible region (34). Whether Lu/BCAM binds preferentially to laminin under its monomeric or dimeric form is not known. Nevertheless, dimerization of Lu/BCAM does not seem to hinder binding to laminin as surface plasmon resonance experiments showed a high affinity between laminin 511/521 and soluble dimers of Lu-Fc chimeras composed of Lu/BCAM extracellular domain fused to the human immunoglobulin Fc fragment that drives dimerization (33, 35). Thus, Lu/BCAM dimers might be the active form needed for laminin binding or might bind laminin with higher affinity than the monomeric form as it was shown for ICAM-1 dimers binding to integrin $\alpha L\beta 2$ (36). This is supported by our functional cellular experiments showing the importance of these dimers for cell migration on a laminin-coated surface. Several adhesion molecules of the IgSF are known to form dimers that are critical for their adhesion and migration functions. Cis-dimerization of CD146 and JAM-A regulates adhesion and migration of endothelial and epithelial cells, respectively (37, 38). In contrast to CD146 (39) and JAM-A (38), Lu/BCAM does not seem to modulate cell migration on laminin 521 by down-regulating integrins but rather by modulating their binding to laminin, weakening firm adhesion and promoting migration (29).

Our findings support the role of Lu/BCAM in inducing cell migration and further identify dimerization and phosphorylation as novel mechanisms through which it operates to sustain this action. Dimerization and phosphorylation are concomitantly needed to induce cell migration as cells expressing the long isoform Lu migrated faster than those expressing the short

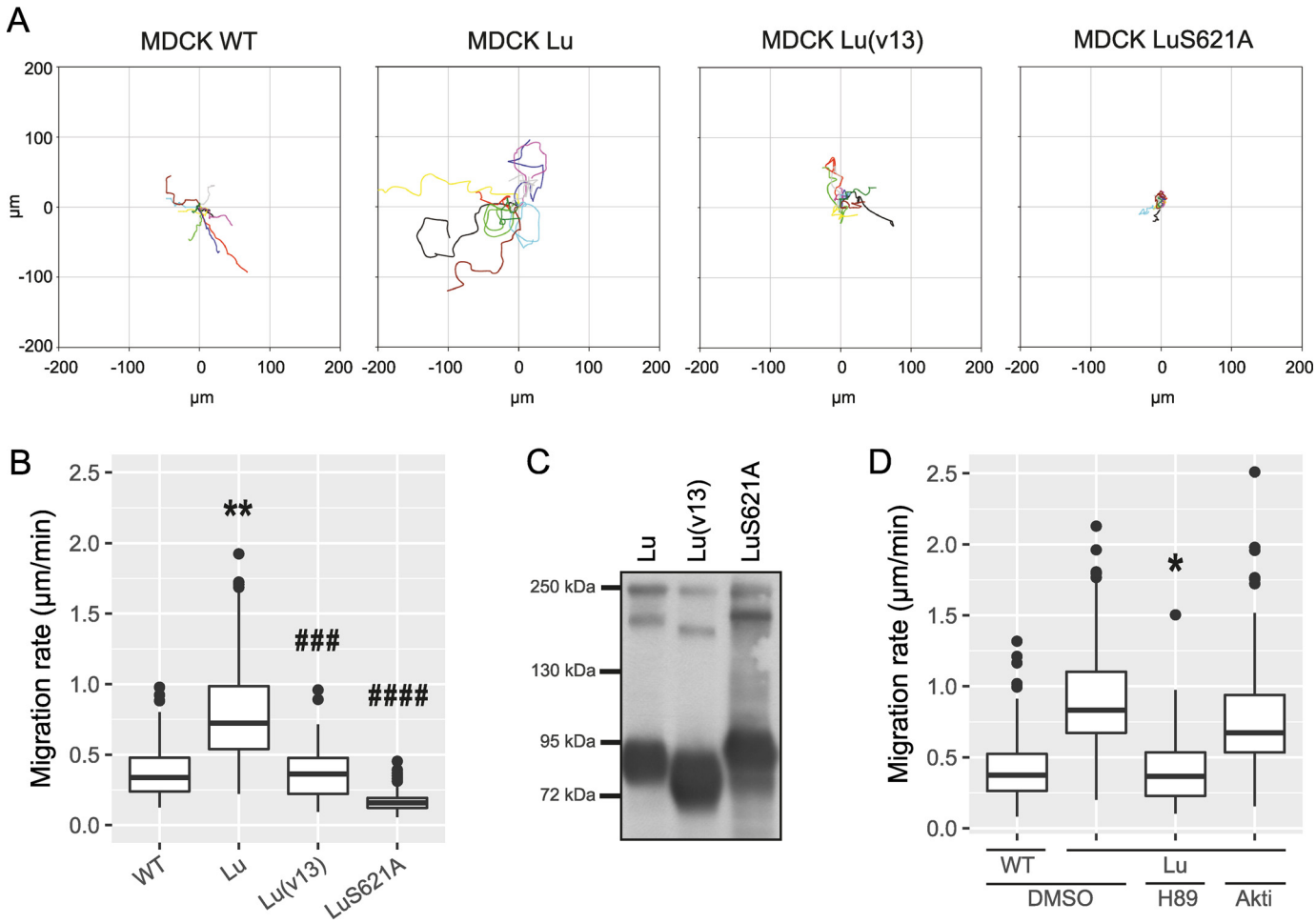

Figure 5. Phosphorylation of Lu serine 621 is necessary for cell migration. Indicated cells were plated in channels coated with laminin 521 and monitored as in Fig. 4. *A*, representative tracks of 10 cells for each cell line over a span of 4 h. *B*, quantification of cell motility as evaluated by cell mean velocity (μm/min) on data collected from three independent experiments. ANOVA was performed on log-transformed data, followed by Tukey's honest significance test. **, $p \leq 0.01$ *versus* MDCK WT cells; ###, $p \leq 0.001$ *versus* MDCK-Lu cells; ####, $p \leq 0.0001$ *versus* MDCK-Lu cells (WT, $n_1 = 44$, $n_2 = 39$, $n_3 = 44$; Lu, $n_1 = 46$, $n_2 = 29$, $n_3 = 43$; Lu(v13), $n_1 = 44$, $n_2 = 36$, $n_3 = 46$; LuS621A, $n_1 = 45$, $n_2 = 34$, $n_3 = 44$). *C*, immunoprecipitated Lu, Lu(v13), and LuS621A from transfected MDCK cells after biotinylation of surface proteins. SDS-PAGE was performed under nonreducing conditions; proteins were detected using streptavidin-HRP ($n = 5$). *D*, quantification of migration rate (μm/min) of MDCK WT and MDCK-Lu cells treated with the PKA inhibitor H89, the Akt inhibitor Akti, or DMSO alone. Data collected from three independent experiments. ANOVA was performed for the MDCK-Lu cells on log-transformed data, followed by Tukey's honest significance test. *, $p \leq 0.05$ *versus* MDCK-Lu DMSO (WT DMSO, $n_1 = 45$, $n_2 = 45$, $n_3 = 50$; Lu DMSO, $n_1 = 36$, $n_2 = 45$, $n_3 = 40$; Lu H89, $n_1 = 48$, $n_2 = 45$, $n_3 = 36$; Lu Akti, $n_1 = 42$, $n_2 = 45$, $n_3 = 40$).

isoform Lu(v13), which forms dimers but is not phosphorylated. In addition, we mapped serine 621 of Lu as the phosphorylation target site of PKA that is involved in MDCK cell migration. Phosphorylation of this serine had been described to support adhesion of red blood cells in sickle cell disease (32) and polycythemia vera (11) through a PKA- and an Akt-dependent pathway, respectively, and here we reveal its novel role in sustaining the migration of epithelial cells. We believe that serine 621 is the only residue involved in the PKA-induced migration as its substitution into alanine in the same MDCK cell line abolishes the cAMP-induced phosphorylation of Lu (32).

Our results on Lu-mediated migration are in accordance with previous studies performed with human fibrosarcoma cell lines overexpressing Lu or with hepatocellular carcinoma cells (29, 40). Lu expression has also been shown to mediate motility on biliary cells in a liver injury context (27). Nevertheless, although our results showing that Lu(v13) does not sustain cell migration are in accordance with the suggested suppressive oncoprotein role of this isoform (41) they are different from those reported by Kikkawa *et al.* (29), showing a migration function for this isoform, although slightly lower than for Lu. This discrepancy might arise from differences in the cell lines used in both studies or from the number of tracked cells in the migration assays, as in our experiments we tracked a much higher number of cells (more than 40 cells in triplicate *versus* 10 cells in Ref. 29). Our results highlight the importance of the relative expression of Lu and Lu(v13) as the Lu/Lu(v13) ratio at the cell surface may control the balance between cellular firm adhesion and migration.

The observation that both Lu/BCAM isoforms form homodimers indicates that the dimerization sites are comprised within the 588 amino acids that are common between Lu and Lu(v13). To gain insights into the structural properties of Lu/BCAM we performed *in silico* modeling analyses. The single transmembrane region was analyzed through different prediction approaches (see "Experimental procedures") to determine

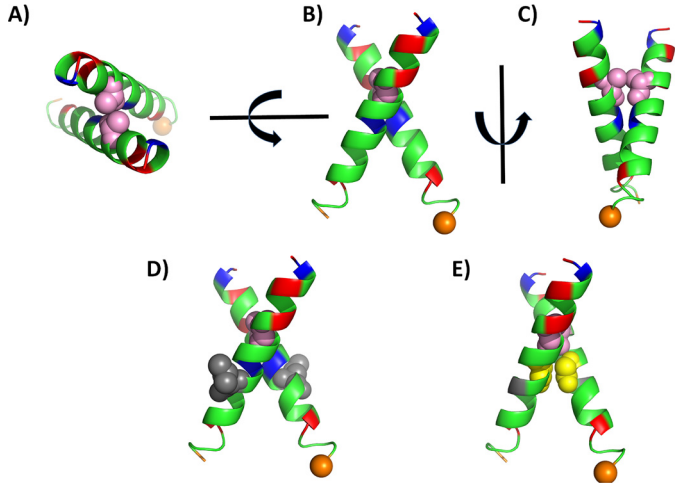

Figure 6. Molecular modeling of the transmembrane dimerization region of Lu/BCAM. *A–C*, the transmembrane helices are shown in three orientations: from the top (*A*) and the side (*B*) with a rotation of 90° (*C*). Alanine 555 residues are represented as *pink spheres*, the other alanine residues are in *red*, glycine residues are in *blue*; the *orange sphere* at the C-terminal end represents cysteine 570. *D* and *E*, structure of the transmembrane helices of LuG559V (*D*) and LuS557V (*E*) mutants in which valine 559 and 557 residues are represented as *gray* and *yellow spheres*, respectively.

the most probable residues incorporated in the lipid bilayer. Predicted residue positions were consistent with those found in the literature (549–570) (42). Prediction of dimeric regions within the transmembrane domain of Lu WT was performed combining two specific methods: LIPS (LIPid-facing Surface) (43) and PREDDIMER (44). LIPS is dedicated to the prediction of helix-lipid interfaces, enabling identifying residues exposed to lipids or involved in helix interactions. The LIPS approach underlined mainly the importance of contact between the two alanine residues at position 555. The PREDDIMER analysis generated 10 different dimeric conformations of which 3 presented the contact constraint at alanine 555 defined by LIPS. Fig. 6, *A* to *C* shows the best-selected solution of the dimerization state in three orientations; it is a classic right-handed dimer. Structural prediction for both LuS557V and LuG559V mutants provided the same dimeric conformation, indicating that the point mutations do not modify the interaction between the two transmembrane helices, further supporting our biochemical results. Indeed, for LuG559V, the side-chain of valine at position 559 is exposed to the lipid bilayer and does not interfere with the dimer docking surface (Fig. 6*D*). As for LuS557V, the side-chain of valine at position 557 is oriented toward the dimer interface but has a neutral effect because it does not interfere with the docking of LuS557V monomers (Fig. 6*E*).

FRET and PLA experiments supported the presence of Lu homodimers at the cell surface. As expected, the FRET efficiency of Lu WT was lower than the positive control (Cit-Cer tandem) as it is underestimated by 50% because of experimental limitation. As a matter of fact, Lu-Cit-Lu-Cit and Lu-Cer-Lu-Cer homodimers do form at the cell surface but are not detected in the assay (25% of total dimers for each subtype). Similarly, the PLA assay also underestimates the dimerization of Lu WT because homodimers that bind two F241-P (25%) or two F241-M (25%) antibodies do not generate fluorescent dots. FRET and PLA results were in accordance with the immunoprecipitation results of Lu WT, LuS557V, and LuG559V. In contrast, although LuC/S-CC/AA dimers were not detected after immunoprecipitation, PLA experiments showed the presence of fluorescent dots for this mutant. The number of dots associated with LuC/S-CC/AA was significantly lower than for Lu WT but higher than for the negative control (MDCK WT, not shown) indicating the presence of low amounts of LuC/S-CC/AA dimers at the cell surface. One explanation is that LuC/S-CC/AA is still able to form some dimers at the cell surface that are dissociated after cell lysis because of the absence of disulfide bonds. The potential presence of such dimers does not seem to support cell migration, strongly suggesting that covalent stabilization of Lu dimers is critical for their mediated migration function.

The absence of Lu dimers in the presence of β-mercaptoethanol and the abrogation of dimerization of the LuC/S-CC/AA mutant support the presence of at least one disulfide bond within each dimer involving one of the three cysteines of each monomer. We performed structural and sequence analyses to evaluate this hypothesis (see "Experimental procedures"). Protein structural analysis indicated that cysteine 570, which is at the boundary of the transmembrane and cytoplasmic domains, is the less likely to form disulfide bonds. To determine the putative cysteine involved in such bonds we studied the evolution of this cytoplasmic region using multiple sequence analyses. We performed a mining of the UniProt/Swiss-Prot database using PSI-BLAST and found more than 400 conserved sequences with appropriate similarity. Interestingly, cysteine 570 was found in all mammals but not in some reptiles. The two other cysteines, cysteine 578 and cysteine 579, were found in all mammals with complete conservation. In the reptile species, it was difficult to distinguish cysteine 578 from cysteine 579 as the local similarity decreased. In contrast, analyzing the sequence from *Ornithorhynchus anatinus*, which has only one cysteine at this position and a high similarity with the human sequence, indicated that cysteine 578 was the conserved residue, suggesting that this cysteine is most probably the residue involved in disulfide bonds within Lu dimers.

In summary, our findings show that Lu/BCAM molecules form dimers at the cell surface and reveal a novel mechanism regulating Lu/BCAM-mediated adhesion and migration of epithelial cells. Further studies of this mechanism could be of interest both in pathological situations, such as cancer cell migration and abnormal red cell adhesion, and in normal physiology during development and tissue formation.

Experimental procedures

Antibodies

Mouse anti-human Lu/BCAM monoclonal antibody (mAb), clone F241, was produced in our institute (32). Human anti-Lu^a mAb, clone 4G11, was produced as described (31). Biotinylated goat polyclonal anti-Lu/BCAM antibody (Ab) was from R&D Systems.

Expression vectors and site-directed mutagenesis

Lu^a, Lu^b, and Lu^b(v13) cDNAs were cloned into the pcDNA3 expression vector as described (45). Mutated forms of Lu^b were

obtained using site-directed mutagenesis as described previously (46). Primers used for the S621A mutation (+1 is taken as the methionine residue of the initiation codon) are already described (46). Primers used for the other mutants are (mutated nucleotides are underlined): for LuS557V, forward 5′-CATGGCCGTGGCCGTCGTCGTGGGCCTCCTGCTCCTCG-3′, reverse 5′-CGAGGAGCAGGAGGCCCACGACGACGGCCACGGCCATG-3′; for LuG559V, forward 5′-CGTGGCCGTCAGCGTGGTCCTCCTGCTCCTCGTCG-3′, reverse 5′-CGACGAGGAGCAGGAGGACCACGCTGACGGCCACG; LuC/S-CC/AA mutant was obtained using 2 steps, first cysteine 570 was mutated into serine, forward 5′-GTTGCTGTCTTCTACAGCGTGAGACGCAAAGG-3′, reverse 5′-CCTTTGCGTCTCACGCTGTAGAAGACAGCAAC-3′; then CC578–579 were mutated into alanine, forward 5′-CGCAAAGGGGGCCCCGCCGCCCGCCAGCGGCGGGAG-3′, reverse 5′-CTCCCGCCGCTGGCGGGCGGCGGGGCCCCCTTTGCG-3′.

Cell culture, transfection, and flow cytometry

MDCK (ATCC), HEK 293T (ATCC) and Caco-2 (DSMZ) cells were grown in DMEM GlutaMAX I supplemented with 10% (MDCK, HEK 293T) or 20% (Caco-2) FCS, antibiotic/antimycotic and 0.1 mM nonessential amino acids. Cells were grown in a humidified atmosphere at 37 °C with 5% CO_2. Stable MDCK and Caco-2 cells expressing WT or mutant Lu/BCAM were obtained as described (32).

Cell surface expression of Lu/BCAM was analyzed using anti-Lu/BCAM F241 mAb followed by a phycoerythrin-conjugated anti-mouse IgG (H+L) (Beckman Coulter); a BD FACSCanto II flow cytometer (Becton Dickinson) with FACSDiva software (version 6.1.2) for acquisition and FlowJo v10 software for data analysis. Expression of Lu WT and dimerization mutant forms in Lu-positive MDCK cells fell within the same range except for LuS557V (Fig. S3*A*); expression of Lu(v13) and LuS621A mutant were similar and higher than Lu WT (Fig. S3*B*).

Protein biotinylation and Western blotting

Cells were washed twice with ice-cold PBS with 1 mM calcium and magnesium (PBS-CM) and incubated with 0.5 mg/ml EZ-Link Sulfo-NHS-LC-Biotin (Pierce) in 10 mM Hepes, pH 7.3–7.6, 150 mM NaCl, 0.2 mM $CaCl_2$, and 0.2 mM $MgCl_2$ for 30 min at 4 °C. Cells were washed twice with PBS-CM and incubated with 10 mM glycine in PBS for 10 min at 4 °C to quench free biotin. After two extra washes with PBS-CM, cells were lysed for 40 min on ice in lysis buffer (10 mM Tris/HCl, pH 7.4, 150 mM NaCl, 1 mM $MgCl_2$, 1 mM $CaCl_2$, and 1% Triton X-100 supplemented with a protease inhibitor mixture (cOmplete, EDTA-free, Roche) and 1 mM PMSF). Cell lysates were centrifuged for 20 min at 11,000 × *g*, and supernatants were precleared with Protein A Sepharose CL-4B beads (GE Healthcare Life Sciences) supplemented with goat serum during 3 h. Following centrifugation at 5000 × *g* for 20 min, Lu/BCAM was immunoprecipitated from supernatants overnight at 4 °C using F241 mAb coupled to Protein A Sepharose beads. After washing the beads five times with the lysis buffer, immunoprecipitated proteins were eluted with Laemmli buffer and analyzed by SDS-PAGE (8% gels), membrane transfer, and chemiluminescence after incubation with horseradish peroxidase-conjugated streptavidin (Life Technologies).

FRET experiments

Lu isoform was expressed as a fusion protein with two different tags: citrine (Cit) and cerulean (Cer). A pEGFP-N2 vector containing Lu cDNA between the BglII (5′ end) and EcoRI (3′ end) restriction sites was used as a backbone. The cDNA sequence encoding the GFP tag was excised by a double EcoRI/NotI digestion and replaced by PCR products digested by the same enzymes encoding either citrine or cerulean, which were amplified from pECitrineFP-C1 or pECeruleanFP-C1vectors using the following primers: forward 5′-GGCCGAATTCATGGTGAGCAAGGGCGAGG-3′ and reverse 5′-CCGGCGGCCGCTCATCACTTGTACAGCTCGTCCATGC-3′. The vector encoding the citrine-cerulean tandem protein was obtained by cloning the cerulean cDNA in the pECitrineFP-C1 vector using the following primers: forward 5′-GGCCGAATTCTGGAGGAGGAGGAATGGTGAGCAAGGGCGAG-3′ and reverse 5′-CCGGGGATCCTCATCACTTGTACAGCTCGTCCATGC-3′ between the restriction sites EcoRI and BamHI. ICAM-4/LW was expressed as a fusion protein with cerulean. The vector encoding the Cit-Cer tandem was used to clone ICAM-4 cDNA. The citrine tag was excised by a NheI/XhoI double digestion and replaced by ICAM-4 cDNA, digested with the same enzymes, amplified from corresponding vector using the following primers: 5′-GGCCGCTAGCATGGGGTCTCTGTTCCCTCTG-3′ and reverse 5′-GGCCCTCGAGCCGCCTGGGACTTCATAGCTA-3′.

HEK 293T cells grown on glass coverslips were transfected with 1 μg of plasmid DNA using FuGENE® 6 Transfection Reagent (Promega). After 36 h cells were fixed with 4% paraformaldehyde in PBS for 20 min at room temperature, washed with PBS, and mounted in ProLong® reagent (Life Technologies). FRET Acceptor bleaching experiments were performed between Cer and Cit. FRET acquisition and measurement were done using a Leica SP5 confocal microscope using the FRET AB wizard (Leica Microsystems). Excitation and emission wavelengths were 405 and 428–487 nm, respectively, for Cer/donor channel; 514 and 532–592 nm, respectively, for Cit/acceptor channel; and 405 and 532–592 nm, respectively, for the FRET channel. Microscope acquisition was done using a 63 × 1.4 NA oil immersion objective (Leica Microsystems). Maximum laser power (65 milliwatt multi-Argon laser) and zoom bleach option were used to bleach the Acceptor (Cit). Pre- and post-bleached images were acquired at 1000 Hz speed, 1024 × 1024 pixels (pixel size 160 nm), and a pinhole set at 1 airy unit. FRET image analysis was done using FRET Acceptor photobleaching (AB) in LASAF software (Leica Microsystems). All fluorescence values were corrected for background noise. The energy transfer efficiency was quantified as follow: FRETeff = (Dpost-Dpre)/Dpost, where Dpost is the fluorescence intensity of the donor after photobleaching and Dpre is the fluorescence intensity of the donor before photobleaching. Several control experiments have been performed under the same experimental condition: Tandem with Cer and Cit (positive control), Cer and Cit, Lu-Cit and Cer, and Lu-Cit and ICAM4-Cer.

Proximity ligation assay

Anti-Lu mAb F241 was conjugated to the PLUS (F241-P) or MINUS (F241-M) oligo arms using the Duolink® In Situ Probemaker PLUS or MINUS kits (Sigma), respectively. MDCK cells were seeded at 500×10^3 cells/30 μl/channel in ibiTreat μ-Slide VI$^{0.4}$ chambers (ibidi) and grown for 24 h in complete medium. Cells were fixed with 4% paraformaldehyde in PBS for 20 min at room temperature and PLA assays were performed using Duolink® In Situ Detection Reagents Red kit (Sigma), following the manufacturer instructions. Briefly, cells were incubated in blocking solution for 30 min at room temperature before incubation with F241-P (negative control) or F241-M (negative control) or both antibodies for 1 h at room temperature. After a washing step with PBS, ligation and amplification steps were performed, cells were washed, and Duolink® *In Situ* Mounting Medium with DAPI was added in the channels. Cells were imaged using a laser scanning confocal microscope (LSM700, Carl Zeiss). Acquired images were then processed using ImageJ (National Institutes of Health) to count the number of spots per field of acquisition using the following steps: maximum intensity projection along *z* axis, subtract background, smooth and find maxima to count the number of spots. The number of nuclei per field of view was determined manually. Data were processed using Excel software (Microsoft) to calculate the ratio "number of spots/nucleus" for each experimental condition.

Cell migration assays

For cell migration on coated laminin, untreated μ-Slide VI$^{0.4}$ chambers (ibidi) were coated with human recombinant LN-521 (Biolamina) at 2 μg/cm^2 and blocked with 1% BSA. MDCK cells were seeded at 2.25×10^3 cells/30 μl/channel to ensure a surface with sparse cells and grown for 3 h in complete medium. Cells were then incubated at 37 °C in FCS-depleted DMEM GlutaMAX I medium for 1 h in a CO_2 microscope stage incubator before monitoring cell migration by time-lapse microscopy, without medium change. Bright field pictures composed of 2×2 mosaics were taken with 10-min intervals for 12 h at 37 °C and 5% CO_2 using an AxioObserver Z1 microscope (Objective 10×) and AxioVision 4 software (Carl Zeiss). For the inhibition assays, cells were treated with the PKA inhibitor H89 (Sigma 19–141, 10 μM), the Akt inhibitor Akti (Sigma A6730, 2.5 μM) in depleted medium and bright field pictures were taken for 5 h at 37 °C and 5% CO_2 using a Celldiscoverer 7 microscope and Zen Blue software (Carl Zeiss). Images were processed with ZEN lite (blue edition) software (Carl Zeiss), and the position of nuclei was tracked using the MTrackJ plugin (47) of Fiji (48) to quantify cell motility; velocities were expressed in μm/min. For each condition, cells were tracked from three different fields (12–15 cells/field). Cells undergoing mitosis were excluded. Randomly selected cells' paths were plotted with SigmaPlot software (Systat Software Inc.) for illustrative purposes.

Protein structural analyses

Different prediction methods were used to define precisely the transmembrane domain of Lu/BCAM, *e.g.* HMMTOP (http://www.enzim.hu/hmmtop/) (49, 57) and TMHMM (http://www.cbs.dtu.dk/services/TMHMM/) (50).[4] The transmembrane segment (in a large window (positions 549 to 570)) was used to predict the potential dimerization using PREDDIMER (http://model.nmr.ru/preddimer/)[4] (44). The sequences from Lu WT and the two mutants (LuS557V and LuG559V) were tested. The methodology LIPS (http://gila.bioe.uic.edu/lab/lips/)[4] was used to define potential important interaction(s) in the transmembrane region of the homodimer (43).

Protein sequence analyses

Using the transmembrane and the cytoplasmic regions, a mining was done with PSI-BLAST (http://blast.ncbi.nlm.nih.gov/)[4] classic approach (51) on UniProt/Swiss-Prot database (52). The selected sequences were aligned using Clustal Omega (http://www.ebi.ac.uk/Tools/msa/clustalo/)[4] webserver (53, 58). The sequences were conserved when they had an e-value higher than 10^{-4} and a coverage higher than 80%.

Statistical analyses

Descriptive analyses and statistical hypothesis testing were performed using R software on RStudio (54, 55). For FRET and PLA analyses, Kruskal-Wallis one-way ANOVA on ranks test was performed, followed by Dunn's multiple comparison procedure in case of differences at a 0.05 significance level. For the migration assays, normal, log-transformed data were used to fit a two-factor (transfectant and experiment or treatment and experiment) linear model. The most influential points (according to the Cook's distance), all of them classified as potential outliers (with absolute studentized residuals values >2.5) were removed to achieve homoscedasticity ($p > 0.05$ on Bartlett's test). This led to removal of 6, 5, and 1 outliers for each analysis (Figs. 4, 5*B*, and 5*D*, respectively). Statistical hypothesis testing was performed by the Tukey post hoc test after analysis of variance.

Author contributions—A. G. and O. R. data curation; A. G., S. C., O. R., and A. G. d. B. formal analysis; A. G. and W. E. N. validation; A. G., O. R., A. G. d. B., and W. E. N. investigation; A. G., S. C., O. R., A. G. d. B., and W. E. N. methodology; A. G., O. R., A. G. d. B., and W. E. N. writing-original draft; A. G. and W. E. N. project administration; A. G., S. C., O. R., Y. C., C. L. V. K., A. G. d. B., and W. E. N. writing-review and editing; W. E. N. conceptualization; W. E. N. supervision; W. E. N. funding acquisition.

Acknowledgments—We acknowledge the Indo-French Centre for the Promotion of Advanced Research/CEFIPRA for Collaborative Grant 5302-2. This work was supported by institutional funding to the Inserm unit 1134, Institut National de la Transfusion Sanguine, Agence Nationale de la Recherche (SCADHESION 2007), and Région Ile-de-France (SESAME 2007 no. F-08-1104/R).

References

1. Bony, V., Gane, P., Bailly, P., and Cartron, J. P. (1999) Time-course expression of polypeptides carrying blood group antigens during human erythroid differentiation. *Br. J. Haematol.* **107,** 263–274 CrossRef Medline

[4] Please note that the JBC is not responsible for the long-term archiving and maintenance of this site or any other third party hosted site.

2. El Nemer, W., Gane, P., Colin, Y., Bony, V., Rahuel, C., Galactéros, F., Cartron, J. P., and Le Van Kim, C. (1998) The Lutheran blood group glycoproteins, the erythroid receptors for laminin, are adhesion molecules. *J. Biol. Chem.* **273,** 16686–16693 CrossRef Medline
3. Udani, M., Zen, Q., Cottman, M., Leonard, N., Jefferson, S., Daymont, C., Truskey, G., and Telen, M. J. (1998) Basal cell adhesion molecule/lutheran protein. The receptor critical for sickle cell adhesion to laminin. *J. Clin. Invest.* **101,** 2550–2558 CrossRef Medline
4. El Nemer, W., Colin, Y., and Le Van Kim, C. (2010) Role of Lu/BCAM glycoproteins in red cell diseases. *Transfus. Clin. Biol.* **17,** 143–147 CrossRef Medline
5. Bartolucci, P., Chaar, V., Picot, J., Bachir, D., Habibi, A., Fauroux, C., Galactéros, F., Colin, Y., Le Van Kim, C., and El Nemer, W. (2010) Decreased sickle red blood cell adhesion to laminin by hydroxyurea is associated with inhibition of Lu/BCAM protein phosphorylation. *Blood* **116,** 2152–2159 CrossRef Medline
6. Chaar, V., Picot, J., Renaud, O., Bartolucci, P., Nzouakou, R., Bachir, D., Galactéros, F., Colin, Y., Le Van Kim, C., and El Nemer, W. (2010) Aggregation of mononuclear and red blood cells through an $\alpha 4\beta 1$-Lu/basal cell adhesion molecule interaction in sickle cell disease. *Haematologica* **95,** 1841–1848 CrossRef Medline
7. Chaar, V., Laurance, S., Lapoumeroulie, C., Cochet, S., De Grandis, M., Colin, Y., Elion, J., Le Van Kim, C., and El Nemer, W. (2014) Hydroxycarbamide decreases sickle reticulocyte adhesion to resting endothelium by inhibiting endothelial lutheran/basal cell adhesion molecule (Lu/BCAM) through phosphodiesterase 4A activation. *J. Biol. Chem.* **289,** 11512–11521 CrossRef Medline
8. El Nemer, W., Gauthier, E., Wautier, M. P., Rahuel, C., Gane, P., Galactéros, F., Wautier, J. L., Cartron, J. P., Colin, Y., and Le Van Kim, C. (2008) Role of Lu/BCAM in abnormal adhesion of sickle red blood cells to vascular endothelium. *Transfus. Clin. Biol.* **15,** 29–33 CrossRef Medline
9. Picot, J., Goudot, C., Berkenou, J., Galacteros, F., Colin, Y., Bartolucci, P., and le van Kim, C. (2014) Flow cytometry analyses reveal association between Lu/BCAM adhesion molecule and osteonecrosis in sickle cell disease. *Am. J. Hematol.* **89,** 115–117 CrossRef Medline
10. Gauthier, E., El Nemer, W., Wautier, M. P., Renaud, O., Tchernia, G., Delaunay, J., Le Van Kim, C., and Colin, Y. (2010) Role of the interaction between Lu/BCAM and the spectrin-based membrane skeleton in the increased adhesion of hereditary spherocytosis red cells to laminin. *Br. J. Haematol.* **148,** 456–465 CrossRef Medline
11. De Grandis, M., Cambot, M., Wautier, M. P., Cassinat, B., Chomienne, C., Colin, Y., Wautier, J. L., Le Van Kim, C., and El Nemer, W. (2013) JAK2V617F activates Lu/BCAM-mediated red cell adhesion in polycythemia vera through an EpoR-independent Rap1/Akt pathway. *Blood* **121,** 658–665 CrossRef Medline
12. Wautier, M. P., El Nemer, W., Gane, P., Rain, J. D., Cartron, J. P., Colin, Y., Le Van Kim, C., and Wautier, J. L. (2007) Increased adhesion to endothelial cells of erythrocytes from patients with polycythemia vera is mediated by laminin α_5 chain and Lu/BCAM. *Blood* **110,** 894–901 CrossRef Medline
13. Novitzky-Basso, I, Spring, F., Anstee, D., Tripathi, D., and Chen, F. (2018) Erythrocytes from patients with myeloproliferative neoplasms and splanchnic venous thrombosis show greater expression of Lu/BCAM. *Int. J. Hematol.* **40,** 473–477 CrossRef Medline
14. Franco, M., Collec, E., Connes, P., van den Akker, E., Billette de Villemeur, T., Belmatoug, N., von Lindern, M., Ameziane, N., Hermine, O., Colin, Y., Le Van Kim, C., and Mignot, C. (2013) Abnormal properties of red blood cells suggest a role in the pathophysiology of Gaucher disease. *Blood* **121,** 546–555 CrossRef Medline
15. Aumailley, M., Bruckner-Tuderman, L., Carter, W. G., Deutzmann, R., Edgar, D., Ekblom, P., Engel, J., Engvall, E., Hohenester, E., Jones, J. C., Kleinman, H. K., Marinkovich, M. P., Martin, G. R., Mayer, U., Meneguzzi, G., *et al.* (2005) A simplified laminin nomenclature. *Matrix Biol.* **24,** 326–332 CrossRef Medline
16. Durbeej, M. (2010) Laminins. *Cell Tissue Res.* **339,** 259–268 CrossRef Medline
17. Garinchesa, P., Sanzmoncasi, M., Campbell, I., and Rettig, W. (1994) Non-polarized expression of basal-cell adhesion molecule B-CAM in epithelial ovarian cancers. *Int. J. Oncol.* **5,** 1261–1266 CrossRef Medline
18. Rettig, W. J., Garin-Chesa, P., Beresford, H. R., Oettgen, H. F., Melamed, M. R., and Old, L. J. (1988) Cell-surface glycoproteins of human sarcomas: Differential expression in normal and malignant tissues and cultured cells. *Proc. Natl. Acad. Sci. U.S.A.* **85,** 3110–3114 CrossRef Medline
19. Rahuel, C., Le Van Kim, C., Mattei, M. G., Cartron, J. P., and Colin, Y. (1996) A unique gene encodes spliceoforms of the B-cell adhesion molecule cell surface glycoprotein of epithelial cancer and of the Lutheran blood group glycoprotein. *Blood* **88,** 1865–1872 Medline
20. André, M., Le Caer, J. P., Greco, C., Planchon, S., El Nemer, W., Boucheix, C., Rubinstein, E., Chamot-Rooke, J., and Le Naour, F. (2006) Proteomic analysis of the tetraspanin web using LC-ESI-MS/MS and MALDI-FTICR-MS. *Proteomics* **6,** 1437–1449 CrossRef Medline
21. Bernemann, T. M., Podda, M., Wolter, M., and Boehncke, W. H. (2000) Expression of the basal cell adhesion molecule (B-CAM) in normal and diseased human skin. *J. Cutan. Pathol.* **27,** 108–111 CrossRef Medline
22. Boado, R. J., Li, J. Y., and Pardridge, W. M. (2000) Selective Lutheran glycoprotein gene expression at the blood-brain barrier in normal brain and in human brain tumors. *J. Cereb. Blood Flow Metab.* **20,** 1096–1102 CrossRef Medline
23. Chang, H. Y., Chang, H. M., Wu, T. J., Chaing, C. Y., Tzai, T. S., Cheng, H. L., Raghavaraju, G., Chow, N. H., and Liu, H. S. (2017) The role of Lutheran/basal cell adhesion molecule in human bladder carcinogenesis. *J. Biomed. Sci.* **24,** 61 CrossRef Medline
24. Kikkawa, Y., Enomoto-Okawa, Y., Fujiyama, A., Fukuhara, T., Harashima, N., Sugawara, Y., Negishi, Y., Katagiri, F., Hozumi, K., Nomizu, M., and Ito, Y. (2018) Internalization of CD239 highly expressed in breast cancer cells: A potential antigen for antibody-drug conjugates. *Sci. Rep.* **8,** 6612 CrossRef Medline
25. Kikkawa, Y., Sudo, R., Kon, J., Mizuguchi, T., Nomizu, M., Hirata, K., and Mitaka, T. (2008) Laminin $\alpha 5$ mediates ectopic adhesion of hepatocellular carcinoma through integrins and/or Lutheran/basal cell adhesion molecule. *Exp. Cell Res.* **314,** 2579–2590 CrossRef Medline
26. Latini, F. R., Bastos, A. U., Arnoni, C. P., Muniz, J. G., Person, R. M., Baleotti, W., Jr., Barreto, J. A., Castilho, L., and Cerutti, J. M. (2013) DARC (Duffy) and BCAM (Lutheran) reduced expression in thyroid cancer. *Blood Cells Mol. Dis.* **50,** 161–165 CrossRef Medline
27. Miura, Y., Matsui, S., Miyata, N., Harada, K., Kikkawa, Y., Ohmuraya, M., Araki, K., Tsurusaki, S., Okochi, H., Goda, N., Miyajima, A., and Tanaka, M. (2018) Differential expression of Lutheran/BCAM regulates biliary tissue remodeling in ductular reaction during liver regeneration. *Elife* **7,** e36572 CrossRef Medline
28. Schön, M., Klein, C. E., Hogenkamp, V., Kaufmann, R., Wienrich, B. G., and Schön, M. P. (2000) Basal-cell adhesion molecule (B-CAM) is induced in epithelial skin tumors and inflammatory epidermis, and is expressed at cell-cell and cell-substrate contact sites. *J. Invest. Dermatol.* **115,** 1047–1053 CrossRef Medline
29. Kikkawa, Y., Ogawa, T., Sudo, R., Yamada, Y., Katagiri, F., Hozumi, K., Nomizu, M., and Miner, J. H. (2013) The lutheran/basal cell adhesion molecule promotes tumor cell migration by modulating integrin-mediated cell attachment to laminin-511 protein. *J. Biol. Chem.* **288,** 30990–31001 CrossRef Medline
30. Bartolini, A., Cardaci, S., Lamba, S., Oddo, D., Marchiò, C., Cassoni, P., Amoreo, C. A., Corti, G., Testori, A., Bussolino, F., Pasqualini, R., Arap, W., Corà, D., Di Nicolantonio, F., and Marchiò, S. (2016) BCAM and LAMA5 mediate the recognition between tumor cells and the endothelium in the metastatic spreading of KRAS-mutant colorectal cancer. *Clin. Cancer Res.* **22,** 4923–4933 CrossRef Medline
31. Richard, M., Perreault, J., Gane, P., El Nemer, W., Cartron, J. P., and St-Louis, M. (2006) Phage-derived monoclonal anti-Lu. *Transfusion* **46,** 1011–1017 CrossRef Medline
32. Gauthier, E., Rahuel, C., Wautier, M. P., El Nemer, W., Gane, P., Wautier, J. L., Cartron, J. P., Colin, Y., and Le Van Kim, C. (2005) Protein kinase A-dependent phosphorylation of Lutheran/basal cell adhesion molecule glycoprotein regulates cell adhesion to laminin $\alpha 5$. *J. Biol. Chem.* **280,** 30055–30062 CrossRef Medline

33. El Nemer, W., Gane, P., Colin, Y., D'Ambrosio, A. M., Callebaut, I., Cartron, J. P., and Van Kim, C. L. (2001) Characterization of the laminin binding domains of the Lutheran blood group glycoprotein. *J. Biol. Chem.* **276,** 23757–23762 CrossRef Medline
34. Mankelow, T. J., Burton, N., Stefansdottir, F. O., Spring, F. A., Parsons, S. F., Pedersen, J. S., Oliveira, C. L., Lammie, D., Wess, T., Mohandas, N., Chasis, J. A., Brady, R. L., and Anstee, D. J. (2007) The Laminin 511/521-binding site on the Lutheran blood group glycoprotein is located at the flexible junction of Ig domains 2 and 3. *Blood* **110,** 3398–3406 CrossRef Medline
35. Parsons, S. F., Lee, G., Spring, F. A., Willig, T. N., Peters, L. L., Gimm, J. A., Tanner, M. J., Mohandas, N., Anstee, D. J., and Chasis, J. A. (2001) Lutheran blood group glycoprotein and its newly characterized mouse homologue specifically bind α5 chain-containing human laminin with high affinity. *Blood* **97,** 312–320 CrossRef Medline
36. Jun, C. D., Carman, C. V., Redick, S. D., Shimaoka, M., Erickson, H. P., and Springer, T. A. (2001) Ultrastructure and function of dimeric, soluble intercellular adhesion molecule-1 (ICAM-1). *J. Biol. Chem.* **276,** 29019–29027 CrossRef Medline
37. Zheng, C., Qiu, Y., Zeng, Q., Zhang, Y., Lu, D., Yang, D., Feng, J., and Yan, X. (2009) Endothelial CD146 is required for in vitro tumor-induced angiogenesis: The role of a disulfide bond in signaling and dimerization. *Int. J. Biochem. Cell Biol.* **41,** 2163–2172 CrossRef Medline
38. Severson, E. A., Jiang, L., Ivanov, A. I., Mandell, K. J., Nusrat, A., and Parkos, C. A. (2008) Cis-dimerization mediates function of junctional adhesion molecule A. *Mol. Biol. Cell* **19,** 1862–1872 CrossRef Medline
39. Alais, S., Allioli, N., Pujades, C., Duband, J. L., Vainio, O., Imhof, B. A., and Dunon, D. (2001) HEMCAM/CD146 down-regulates cell surface expression of (β)1 integrins. *J. Cell Sci.* **114,** 1847–1859 Medline
40. Enomoto-Okawa, Y., Maeda, Y., Harashima, N., Sugawara, Y., Katagiri, F., Hozumi, K., Hui, K. M., Nomizu, M., Ito, Y., and Kikkawa, Y. (2017) An anti-human Lutheran glycoprotein phage antibody inhibits cell migration on laminin-511: Epitope mapping of the antibody. *PLoS One* **12,** e0167860 CrossRef Medline
41. Akiyama, H., Iwahana, Y., Suda, M., Yoshimura, A., Kogai, H., Nagashima, A., Ohtsuka, H., Komiya, Y., and Tashiro, F. (2013) The FBI1/Akirin2 target gene, BCAM, acts as a suppressive oncogene. *PLoS One* **8,** e78716 CrossRef Medline
42. Parsons, S. F., Mallinson, G., Holmes, C. H., Houlihan, J. M., Simpson, K. L., Mawby, W. J., Spurr, N. K., Warne, D., Barclay, A. N., and Anstee, D. J. (1995) The Lutheran blood group glycoprotein, another member of the immunoglobulin superfamily, is widely expressed in human tissues and is developmentally regulated in human liver. *Proc. Natl. Acad. Sci. U.S.A.* **92,** 5496–5500 CrossRef Medline
43. Adamian, L., and Liang, J. (2006) Prediction of transmembrane helix orientation in polytopic membrane proteins. *BMC Struct. Biol.* **6,** 13 CrossRef Medline
44. Polyansky, A. A., Chugunov, A. O., Volynsky, P. E., Krylov, N. A., Nolde, D. E., and Efremov, R. G. (2014) PREDDIMER: A web server for prediction of transmembrane helical dimers. *Bioinformatics* **30,** 889–890 CrossRef Medline
45. El Nemer, W., Rahuel, C., Colin, Y., Gane, P., Cartron, J. P., and Le Van Kim, C. (1997) Organization of the human *LU* gene and molecular basis of the Lu^a/Lu^b blood group polymorphism. *Blood* **89,** 4608–4616 Medline
46. El Nemer, W., Colin, Y., Bauvy, C., Codogno, P., Fraser, R. H., Cartron, J. P., and Le Van Kim, C. (1999) Isoforms of the Lutheran/basal cell adhesion molecule glycoprotein are differentially delivered in polarized epithelial cells. Mapping of the basolateral sorting signal to a cytoplasmic dileucine motif. *J. Biol. Chem.* **274,** 31903–31908 CrossRef Medline
47. Meijering, E., Dzyubachyk, O., and Smal, I. (2012) Methods for cell and particle tracking. *Methods Enzymol.* **504,** 183–200 CrossRef Medline
48. Schindelin, J., Arganda-Carreras, I., Frise, E., Kaynig, V., Longair, M., Pietzsch, T., Preibisch, S., Rueden, C., Saalfeld, S., Schmid, B., Tinevez, J. Y., White, D. J., Hartenstein, V., Eliceiri, K., Tomancak, P., and Cardona, A. (2012) Fiji: An open-source platform for biological-image analysis. *Nat. Methods* **9,** 676–682 CrossRef Medline
49. Tusnády, G. E., and Simon, I. (2001) The HMMTOP transmembrane topology prediction server. *Bioinformatics* **17,** 849–850 CrossRef Medline
50. Krogh, A., Larsson, B., von Heijne, G., and Sonnhammer, E. L. (2001) Predicting transmembrane protein topology with a hidden Markov model: Application to complete genomes. *J. Mol. Biol.* **305,** 567–580 CrossRef Medline
51. Altschul, S. F., Madden, T. L., Schäffer, A. A., Zhang, J., Zhang, Z., Miller, W., and Lipman, D. J. (1997) Gapped BLAST and PSI-BLAST: A new generation of protein database search programs. *Nucleic Acids Res.* **25,** 3389–3402 CrossRef Medline
52. UniProt Consortium (2015) UniProt: A hub for protein information. *Nucleic Acids Res.* **43,** D204–D212 CrossRef Medline
53. Sievers, F., Wilm, A., Dineen, D., Gibson, T. J., Karplus, K., Li, W., Lopez, R., McWilliam, H., Remmert, M., Söding, J., Thompson, J. D., and Higgins, D. G. (2011) Fast, scalable generation of high-quality protein multiple sequence alignments using Clustal Omega. *Mol. Syst Biol.* **7,** 539 CrossRef Medline
54. R Core Team. (2018) *R: A Language and Environment for Statistical Computing*. R Foundation for Statistical Computing, Vienna, Austria
55. RStudio Team. (2015) *RStudio*: *Integrated Development for R*. RStudio, Inc., Boston, MA
56. Deleted in proof
57. Tusnády, G. E., and Simon, I. (1998) Principles governing amino acid composition of integral membrane proteins: Applications to topology prediction. *J. Mol. Biol.* **283,** 489–506. CrossRef
58. Li, W., Cowley, A., Uludag, M., Gur, T., McWilliam, H., Squizzato, S., Park, Y. M., Buso, N., and Lopez, R. (2015) The EMBL-EBI bioinformatics web and programmatic tools framework. *Nucleic Acids Res.* **43,** W580–W584 CrossRef Medline